Electrical Power and Energy Systems 133 (2021) 107253

Contents lists available at ScienceDirect

International Journal of Electrical Power and Energy Systems

journal homepage: www.elsevier.com/locate/ijepes

Computationally efficient method for placing reactive power sources against contingencies☆

Ahmet Öner, Ali Abur *

Department of Electrical and Computer Engineering, Northeastern University, Boston, MA, United States

ARTICLE INFO

Keywords:
Reactive power compensation
Robust power grid
Voltage problems
Voltage stability

ABSTRACT

This paper presents a computationally efficient algorithm to find the locations and required reactive power injections for a minimum number of reactive power compensators under a set of considered contingencies. The problem is formulated and solved in two stages. The first stage solves the security-constrained DC optimal power flow problem to find the active power generation dispatch. Then, the second stage determines the best locations for a minimum number of reactive power compensators to assist the reactive power generation dispatch in order to maintain bus voltages within limits and to ensure voltage stability under the considered set of contingencies. Effectiveness and computational performance of the proposed method are illustrated by extensive simulations carried out on PEGASE 2869-bus system.

1. Introduction

Power system operators aim to keep the system operating in the normal state such that the power balance between loads and generators is satisfied, bus voltages and power flows are within limits. However, unexpected disturbances such as rapidly varying generation, line switching and faults may disrupt the normal operation of the power system since voltage control parameters such as transformer taps may not be sufficient to resolve the violations caused by these disturbances. The system could transition to insecure normal state or to emergency state due to such unexpected events. Under these scenarios, extreme measures like load shedding may be necessary to maintain voltages within limits and/or to avoid voltage collapse (restorative state). Hence, it is customary to maintain a security margin in order to withstand any unexpected disturbances and maintain a secure and stable operation.

One way is by strategic placement of reactive power compensators such as static VAr compensators (SVCs) and static synchronous compensators (STATCOMs) in the power grid based on the anticipated operating conditions and system contingencies. The benefits of installing shunt flexible AC transmission system (FACTS) devices are well recognized by several investigators in recent years [1–4]. In [1], a case study demonstrated that optimally placed SVCs could significantly improve the economic and reliable operation of power systems with large penetration of wind generation. Another study [2] investigated how the first swing stability limit of a power system could be improved by using FACTS devices such as SVCs and STATCOMs. In [3], FACTS devices are used for reducing the financial losses in the network due to voltage sags. The work presented in [4] used an SVC for controlling voltage in low voltage grids. In [5] SVC locations are determined by using the participation of each load in the critical mode to identify the bus with the highest involvement in voltage collapse. In [6], SVCs are proposed to be located using both a genetic algorithm and modal analysis. While they obtain the same placement results for both methods, the sizing of SVCs are determined by using genetic algorithm because the optimal size of SVCs are unknown in modal analysis. In [7], STATCOMs are placed to enhance the voltage stability based on particle swarm optimization. In [8], SVCs are placed to maximize the loading margin, which can also be associated with voltage stability and bus voltage limits. The problem is formulated as a mixed-integer nonlinear programming problem and solved using Benders decomposition to improve computational performance. The authors of [9] place a predetermined number of SVCs to maximize the reactive margin of the power system with two recursive optimization blocks. The study reported in [10] uses a genetic algorithm to place a predetermined number of SVCs to the grid, but suffers from

☆ The authors are grateful for the partial support provided by the NSF/CRISP Type 2 Grant with Award Number:1638234. This work also made use of Engineering Research Center shared facilities supported by the Engineering Research Center Program of the National Science Foundation and the Department of Energy under NSF Award Number EEC-1041877 and the CURENT Industry Partnership Program.

* Corresponding author. Tel.: +1 617.373.3051.
E-mail addresses: aoner@ece.neu.edu (A. Öner), abur@ece.neu.edu (A. Abur).

https://doi.org/10.1016/j.ijepes.2021.107253
Received 15 November 2020; Received in revised form 24 March 2021; Accepted 8 May 2021
Available online 18 June 2021

heavy computational load especially when applied to large grids. Another study [11] linearizes the nonlinear problem and installs SVCs to maximize photo-voltaic hosting capacity by using mixed-integer linear programming but without guarantees on voltage stability.

As evident from the work presented in [8], the computational burden of optimal placement problem presents a practical limitation for applying it to very large scale systems considering multi-contingency cases. This paper presents a practical and easily implementable solution that will address this limitation. The proposed approach is computationally efficient and applicable to large scale power grids yielding a secure and stable as well as the most cost-effective reactive power compensator placement strategy under considered contingencies.

In general, in system simulations voltage magnitude limits should incorporate a security margin in order to account for numerical approximations in simulations and for differences between actual and simulated operating points [12]. Moreover, the margin should be applied to ensure post-contingency voltage stable solutions.

The proposed approach formulates the problem by first solving only the real power security constrained optimal dispatch problem followed by a reactive power compensator placement problem which accounts for all the considered contingencies. These contingencies may be N-1, N-1–1 or more complex combination of line/generator outages due to forecasted extreme events. While the first stage is formulated and solved via quadratic programming, the second stage places a minimum number of required reactive power compensators and solves the reactive power generation dispatch problem as well as voltage stability problem via mixed-integer linear programming.

The rest of the paper is organized as follows. Formulation and solution of the method are explained in Section 3. Section 4 presents the placement results and validations obtained by applying the developed two-stage approach to PEGASE 2869-bus systems. Section 5 concludes the paper. Before presenting the details of the problem formulation, voltage stability problem will be discussed and the technical innovation, derivation of the stability index, will be presented.

2. Voltage stability index

In this work, the so called voltage stability index, L which is developed and presented in [13] will be used in the problem formulation. Following the suggestion by Sekine in the discussion section of [13], this index will be referred as the *proximity to voltage existence index* in this paper.

The algorithm presented in [13] computes this L-index in three steps. The first step involves identifying the load and generator buses and forming the H-matrix which is built by partitioning and rearranging the network equations as follows:

$$\begin{bmatrix} V_L \\ I_G \end{bmatrix} = [H] \begin{bmatrix} I_L \\ V_G \end{bmatrix} = \begin{bmatrix} Z_{LL} & F_{LG} \\ K_{GL} & Y_{GG} \end{bmatrix} \begin{bmatrix} I_L \\ V_G \end{bmatrix} \tag{1}$$

where:

V_L, I_L: Voltage and injected current vectors at load buses,
V_G, I_G: Voltage and injected current vectors at generator buses,
$Z_{LL}, F_{LG}, K_{GL}, Y_{GG}$: Partitions of H-matrix.

In the sequel, the indices j and i will refer to load and generator buses, respectively.

The second step involves calculation of V_{0j} for load buses using the sub-matrix F in (1) and the voltages at generator buses, V_i:

$$V_{0j} = -\sum_{i \in G} F_{ji} V_i \tag{2}$$

Finally, the voltage stability index L_j is calculated for all load buses as:

$$L_j = \left| 1 + \frac{V_{0j}}{V_j} \right| \tag{3}$$

It is shown in [13] that the system will be voltage stable if L_j remains less than 1.0. Smaller values of L_j will yield more conservative solutions with respect to proximity to voltage instability. As an example, consider Fig. 1 which shows the results obtained by continuation power flow at a PQ bus for three different power factors where, λ is the loading factor that defines the relationship between the load on continuation power flow and the base case load. While the part above the nose point represents voltage stable solutions, a stability margin can be established using the stability index of (3).

$$Load = Load_{base}(\lambda + 1) \tag{4}$$

Note that F_{ji}, V_i, V_j and V_{0j} are complex numbers. Moreover, the magnitude (the absolute value) of the ratio of V_{0j} to V_i is used while calculating L_j, hence, the expression (3) is non-linear. Ensuring voltage stability for all scenarios makes the reactive power source placement problem harder to solve. One way to address this challenge is to find a suitable linearization which will allow its formulation as a mixed-integer linear programming problem that can be rapidly solved. The proposed linearization procedure is explained by the following tutorial example.

2.1. Tutorial example

This simple 3-bus example (with system diagram shown in Fig. 2) will be used to illustrate how the first order linear approximation of the L-index is obtained. Since there are two generation buses and one load bus, the size of F_{ji} and V_i will be 1x2 and 2x1, shown in polar form at (5) and (6), respectively.

$$F_{ji} = [\, a\angle\theta_a \quad b\angle\theta_b \,] \tag{5}$$

$$V_i = \begin{bmatrix} V_1\angle\theta_1 \\ V_2\angle\theta_2 \end{bmatrix} \tag{6}$$

Hence, V_{0j} can be calculated using (2) as below. Here the size of V_{0j} will be 1x1 because there is only one load bus, i.e. bus 3.

$$V_{0j} = -\sum [\, a\angle\theta_a \quad b\angle\theta_b \,] \begin{bmatrix} V_1\angle\theta_1 \\ V_2\angle\theta_2 \end{bmatrix} \tag{7}$$

$$V_{0j} = -aV_1\angle(\theta_a + \theta_1) - bV_2\angle(\theta_b + \theta_2)$$

Now, V_{0j} can be incorporated into (3) to find L-index which should be smaller than one for voltage stability.

$$L_j = \left| 1 - \frac{aV_1\angle(\theta_a + \theta_1) + bV_2\angle(\theta_b + \theta_2)}{V_3\angle\theta_3} \right| \langle 1 \tag{8}$$

where, V_1, V_2, V_3, a and b are real numbers while $\theta_1, \theta_2, \theta_3, \theta_a$ and θ_b are angles. Henceforth, (8) can now be readily linearized.

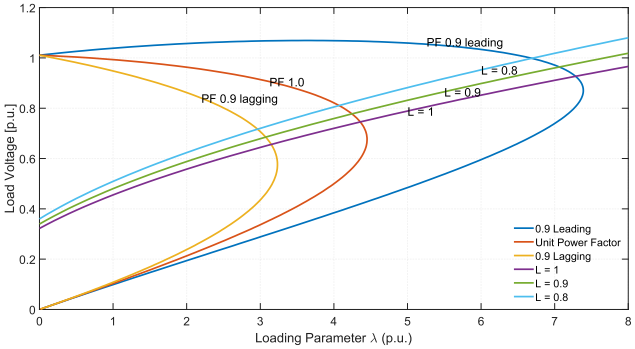

Fig. 1. Continuation power flow example.

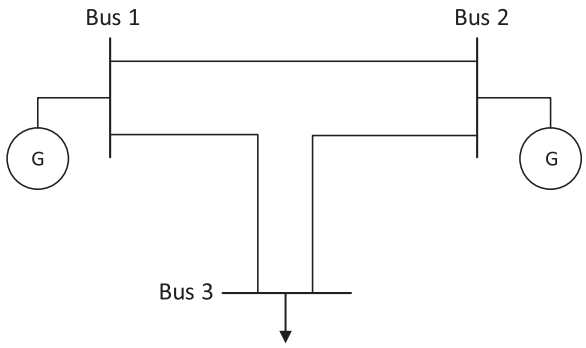

Fig. 2. 3-Bus System.

$$L_j = \left| \frac{V_3 - aV_1\angle(\theta_a + \theta_1 - \theta_3) - bV_2\angle(\theta_b + \theta_2 - \theta_3)}{V_3} \right| \langle 1 \tag{9}$$

$$\underbrace{|V_3 - aV_1\angle\beta_1 - bV_2\angle\beta_2|}_{K} < V_3 \tag{10}$$

where, K is defined as the left hand side of the inequality, β_1 and β_2 are defined as follows for simplification:

$$\beta_1 = \theta_a + \theta_1 - \theta_3 \tag{11}$$

$$\beta_2 = \theta_b + \theta_2 - \theta_3$$

(10) can also be written as a circle inequality:

$$Re(K)^2 + Im(K)^2 < V_3^2 \tag{12}$$

where, $Re(K)$ and $Im(K)$ are the real and imaginary parts of the complex number K, respectively. The inequality is shown with the red circle in Fig. 3, where the feasible region is inside of the circle.

$$Re(K) = V_3 - aV_1 cos\beta_1 - bV_2 cos\beta_2 \tag{13}$$

$$Im(K) = -aV_1 sin\beta_1 - bV_2 sin\beta_2 \tag{14}$$

Also, a polygon can be drawn inside the circle using line segments whose terminal nodes are on the circle, providing a linear approximation of the circle equation. A different linear equation for each line segment of the polygon is derived.

$$Y_1 Re(K) + Y_2 Im(K) + Y_3 V_3 < 0 \tag{15}$$

where, the variables are V_1, V_2 and V_3, and the coefficient vectors are Y_1, Y_2 and Y_3. In Fig. 3, a dodecagon is drawn with twelve blue line segments (dodecagon is a good trade-off between a sufficiently good approximation and decreasing the computational burden). Finally, (15) can be written in the matrix form as below:

$$A \begin{bmatrix} V_1 \\ V_2 \\ V_3 \end{bmatrix} \langle \begin{bmatrix} 0 \\ \vdots \\ 0 \end{bmatrix} \tag{16}$$

Since the mixed-integer linear programming problem will use the square of the voltage magnitude as the variable, another approximation is introduced to replace the voltage magnitude by its square as the unknown. Considering the voltage magnitudes are limited between 0.9 p.u. and 1.1 p.u., the below equation can be written:

$$V = p_1 V^2 + p_2 \tag{17}$$

where, p_1 and p_2 are equal to 0.4997 and 0.4987, respectively and the root mean square error (RMSE) is 0.0015 p.u. Considering the standard deviation of measurement devices in state estimation is around 0.004 p.u. [14], the approximation is considered acceptable.

Substituting V matrix in (16) with (17), it can be rewritten again as below:

$$Ap_1 \begin{bmatrix} V_1^2 \\ V_2^2 \\ V_3^2 \end{bmatrix} \langle -A \begin{bmatrix} p_2 \\ p_2 \\ p_2 \end{bmatrix} \tag{18}$$

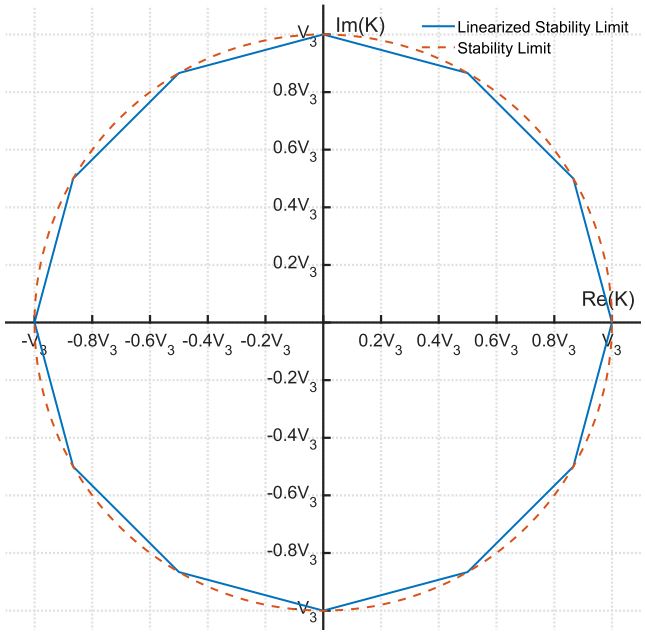

Fig. 3. Polygon approximation of stability limit for the 3-bus system.

3. Problem formulation

Based on the derived L-index in the above section, the reactive power compensator placement problem can now be formulated. The formulation and solution will be carried out in two stages involving quadratic programming and mixed-integer linear programming (MILP) solution tools. The first stage solves the well known security constrained DC optimal power flow problem in order to determine the optimal active power dispatch under all considered contingencies. Then, the second stage minimizes the total number of reactive power compensators required to solve the optimal reactive generation dispatch problem while ensuring voltage stability. The details of these two stages are described in the subsections below.

3.1. Security constrained DC optimal power flow

Security constrained generation dispatch is used in the real-time and day-ahead markets to generate forward dispatch to have reliable system operation. While N-1 criteria are the minimum reliability standard for the grid, much more advanced security constraints can be included representing loss of multiple lines during extreme events. Those conditions may include possible expected outages (line and/or generator outages), and/or sudden changes in generator outputs. Also, historical outage records of utilities can be used to select the contingencies to be considered for this purpose. In order to reduce unnecessary computational load associated with secure contingencies, contingency screening and ranking algorithms can also be used.

While meeting technical and safety requirements, the objective is to find the most economical generation dispatch. The details of the problem formulation, including the objective function and the constraint equations, are described below.

3.1.1. Objective function

The objective is to minimize the total generation cost given by:

$$\min\ a_1 P_G^2 + a_2 P_G + a_3 \tag{19}$$

where, a_1, a_2 and a_3 are the quadratic, linear and the constant coefficient vectors, respectively. P_G is the vector of active power generation.

3.1.2. Constraints

The above objective function will have to be minimized subject to a number of constraints, which are described next.

3.1.2.1. Active power balance equations. Active power balance equations need to be included for every bus i:

$$P_G\left(i\right) - P_D\left(i\right) = \sum_{j=1}^{n_B} P_{ij} \tag{20}$$

where, n_B represents the total number of buses, P_{ij} is the active power flow on branch (i,j). P_D is the vector of active power demand.

Active power flow along branch (i,j) can be expressed as:

$$P_{ij} = B_{ij}\left(\theta_i - \theta_j\right) \tag{21}$$

where, B_{ij} represents the imaginary part of ij^{th} element of the bus admittance matrix. θ_i and θ_j are the phase angles for the buses i and j.

Substituting (21) into (20) yields:

$$P_G - P_D = B\theta \tag{22}$$

Note that the above equation is valid for the base case. Next, consider multiple contingencies where some of the lines and/or generators are removed, and/or generation outputs are reduced at certain buses. The objective is to find an optimal dispatch P_G which will remain viable for all these considered contingencies. This can be accomplished by augmenting (22) with new constraints corresponding to all these contingencies:

$$\begin{array}{l} P_G - P_D = B^1\theta^1 \\ P_G - P_D = B^2\theta^2 \\ \quad\vdots \quad = \quad \vdots \\ P_G - P_D = B^k\theta^k \end{array} \tag{23}$$

where, superscripts 1, 2, …, k represent the contingency indices.

In addition, the total generation should match the total demand:

$$\sum_{i=1}^{n_B}\left(P_G\left(i\right)\right) = \sum_{i=1}^{n_B}\left(P_D\left(i\right)\right) \tag{24}$$

3.1.2.2. Active generator limits. Each generator will have its upper and lower output limits given by:

$$\underline{P} \leqslant P_G \leqslant \overline{P} \tag{25}$$

3.1.2.3. Angle limits. Limits on the phase angle separation between neighboring buses for each contingency will be:

$$\begin{array}{l} \underline{\theta} \leqslant A^1\theta^1 \leqslant \overline{\theta} \\ \underline{\theta} \leqslant A^2\theta^2 \leqslant \overline{\theta} \\ \vdots\leqslant \quad \vdots \quad \leqslant\vdots \\ \underline{\theta} \leqslant A^k\theta^k \leqslant \overline{\theta} \end{array} \tag{26}$$

where, $A^1, A^2, \ldots, A^k$ are the incidence matrices for different contingencies.

Based on the above described equations, the security constrained DC optimal power flow can be solved using quadratic programming with quadratic objective function and linear constraints. While quadratic programming gives an accurate solution on the conservative side, more complex equations could be used for more realistic simulations, such as the value point effect. However, they are ignored for computational efficiency.

$$\min_{\theta^1,\ldots,\theta^k,P_G}\ a_1 P_G^2 + a_2 P_G + a_3 \tag{27}$$

subject to:

1. Active Power Balance Equations given by (23), (24)
2. Active Generator Limits given by (25)
3. Angle Limits given by (26)

3.2. Reactive power compensator placement method

The purpose of reactive power compensator placement is to address the voltage problems, which are caused by the lack of reactive power in the system. While technical feasibility is the main concern, the problem is also formulated in order to accomplish this using a small number of reactive power compensators, hence at minimum overall cost.

The proposed approach exploits the decoupling between the real and reactive power flows by first solving a security constrained DC optimal power flow for the active generation dispatch for all the considered contingencies. Hence, the reactive power compensator placement problem is formulated assuming a known set of active power injections and bus voltage phase angles. The set of unknowns will include the square of bus voltage magnitudes, generator bus reactive power injections, reactive power compensator locations and their reactive power injections. Objective function and associated constraints are described in more detail next.

3.2.1. Objective function

The objective is to place a minimum number of reactive power compensators to minimize the installation cost.

$$\min\ \sum_{i=1}^{n_B} z_i \tag{28}$$

where z_i is a binary variable which is 1 if a reactive power compensator is placed at bus i. Also, the objective function is flexible to write a more complex cost such as cost of reactive power compensator per kVAr.

3.2.2. Constraints

3.2.2.1. Reactive power balance equations. The reactive power flow on branch (i,j) can be expressed as below [15]:

$$Q_{ij} = -b_{ij}\frac{V_i^2 - V_j^2}{2} - g_{ij}\theta_{ij} + Q_{ij,Loss} \tag{29}$$

where, b_{ij} and g_{ij} are susceptance and conductance of branch (i,j), θ_{ij} is phase angle difference between bus i and bus j, and V_i^2 is square of voltage magnitude at bus i. The reactive power loss on branch (i,j), $Q_{ij,Loss}$, can be approximated as:

$$Q_{ij,Loss} = \frac{-b_{ij}}{2}\left(\theta_{ij}^2 + V_{ij}^2\right) \tag{30}$$

where, V_{ij} is voltage magnitude difference between bus i and bus j. Since V_{ij}^2 will typically be much smaller than θ_{ij}^2, V_{ij}^2 can be neglected in (30). Thus, (29) will be linear in V^2.

Considering shunt elements, reactive power balance equations for a given bus i can be written as below:

$$Q_G\left(i\right) - Q_D\left(i\right) = \sum_{j=1}^{n_B} Q_{ij} + \sum_{j=1}^{n_B} - B_{ij}V_i^2 \tag{31}$$

where, Q_G and Q_D are the vectors of reactive power generation and load, respectively. Lastly, reactive power compensator will inject required amount of reactive power for the chosen buses. The reactive power

balance equations will then be modified as:

$$Q_G(i) + Q_P(i) - Q_D(i) = \sum_{j=1}^{n_B} \left(-b_{ij}\frac{V_i^2 - V_j^2}{2} - g_{ij}\theta_{ij} - \frac{b_{ij}}{2}\theta_{ij}^2 \right) + \sum_{j=1}^{n_B} -B_{ij}V_i^2 \tag{32}$$

where, $Q_P(i)$ is the reactive power injection supplied by reactive source at bus i. If bus i is not chosen for the placement, the corresponding reactive injection will be zero.

3.2.2.2. Reactive generator limits. The reactive power generation will have the following limits:

$$\underline{Q_G} \leqslant Q_G \leqslant \overline{Q_G} \tag{33}$$

where, $\underline{Q_G}$ and $\overline{Q_G}$ are the lower and upper limits for the reactive power injection vector.

3.2.2.3. Voltage limits. The square of voltage magnitudes will be bounded as follows:

$$\underline{V_i^2} \leqslant V_i^2 \leqslant \overline{V_i^2} \tag{34}$$

3.2.2.4. Reactive power compensator placement constraints. The binary placement vector, z, and the reactive power injection vector Q_P will be combined to enforce limits on reactive injections as shown below:

$$z\ \underline{Q_P} \leqslant Q_P \leqslant z\ \overline{Q_P} \tag{35}$$

where, $\underline{Q_P}$ and $\overline{Q_P}$ are the lower and upper limits for the reactive power injection vector.

3.2.2.5. Line flow limits. The apparent power flow limits constitute a circular inequality where the radius of the limit circle, $S_{ij,max}$, will represent the line flow limit as given below.

$$P_{ij}^2 + Q_{ij}^2 \leqslant S_{ij,max}^2 \tag{36}$$

Note that it is possible to use a polygon based linearization as shown in [15] to approximate the area of the circle by a polygon:

$$\psi_1 P_{ij} + \psi_2 Q_{ij} + \psi_3 \leqslant 0 \tag{37}$$

where, ψ_1, ψ_2 and ψ_3 are the coefficient matrices that form straight line segments of the polygon. The dimensions of the matrices ψ_1, ψ_2 and ψ_3 are equal to the product of the total number of straight line segments and the total number of branches.

P_{ij} is a constant which can be calculated and substituted into (37) using (21) with known B_{ij} and θ. On the other hand, since Q_{ij} is a function of V^2, Q_{ij} can be replaced by (29).

The reactive power compensator placement problem can now be formulated and solved as a mixed integer programming problem. Since the problem has linear constraints, it is possible to obtain a fast solution even for very large power grids. The problem formulation is shown in compact form below:

$$\begin{matrix} min_{\left(Q_G, V^2, Q_P\right)^1,} & \sum_{i=1}^{n_B} z_i \\ \vdots & \\ \left(Q_G, V^2, Q_P\right)^k, z & \end{matrix} \tag{38}$$

subject to:

1. Reactive Power Balance Equations given by (32)
2. Reactive Generator Limits given by (33)
3. Voltage Limits given by (34)
4. Reactive Power Compensator Placement Constraints given by (35)
5. Line Flow Limits given by (37)
6. Voltage Stability Limits given by (18)

Note that, each contingency case will contribute a corresponding set of constraints and the problem will be solved subject to all of the contingency constraints. The final solution should yield a solution within the limits for all considered contingencies. A block diagram of the proposed strategy is shown in Fig. 4.

4. Simulation results

The proposed method is implemented and tested on PEGASE 2869-bus system [16,17] to verify its applicability for realistic large scale power grids. Both the quadratic programming and mixed-integer linear programming (MILP) problems are solved using the Gurobi Optimizer [18].

Simulation-1:

In order to effectively illustrate the value of the algorithm, outage cases which result in the largest increase in the stability index, L, is determined and used for simulations. While most of the outages do not have a remarkable effect on voltage profiles and voltage instability, a few were found to have significant impact. Therefore, to find the most effective (worst) outage, N-1 contingencies are analyzed for all of 4582 branches and 510 generators using the high-performance computing center facilities. The analysis showed that the outage of the line 1534–100 would have a significant effect on voltage instability (biggest L observed), among all considered N-1 contingencies.

Matpower ACOPF solver [19] failed to yield a converged solution under this contingency when the minimum voltage magnitude is limited to 0.9 p.u. In order to find a feasible solution within the voltage limits, minimum bus voltage limits are decreased by 0.01 p.u. at a time until it gives a feasible solution. In this example, a feasible solution is reached when the limit for minimum voltage is reduced to 0.84 p.u. Table 1 summarizes the minimum voltages for a feasible solution with different loading factors, λ. Also, the biggest voltage stability index and objective function is calculated using the Matpower solutions and placed into Table 1.

Then, the proposed algorithm is executed without stability constraints while minimum bus voltage limits are set as 0.9 p.u. and maximum reactive power injection limits of placed reactive power compensators are set as 400 MVAr. Table 2 summarizes the algorithm results with different loading factors. As expected, the required number of reactive power compensators increases with increasing loading factors.

Table 3 summarizes the algorithm results with different stability margins to guarantee post-contingency voltage stable solutions. As expected, the required number of reactive power compensators are

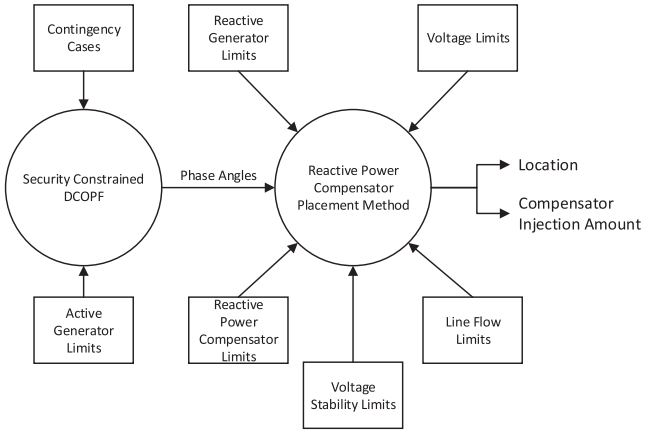

Fig. 4. Block diagram of the proposed strategy.

Table 1
Matpower solutions.

Loading Factor λ	Voltage Limit V_m	Stability Index L	Objective function ($/hr)
0	0.84	0.805	7038207
0.05	0.76	1.0092	8033623
0.1	N/A	N/A	N/A

Table 2
Without stability constraints

Loading Factor λ	Voltage Limit V_m	Stability Index L	Objective function ($/hr)	Number of Reactive Power Compensator Placements
0	0.9	0.5606	6976539	1
0.05	0.9	0.6992	7509578	1
0.1	0.9	0.7284	8127704	1
0.15	0.9	0.7513	8764173	1
0.2	0.9	0.7352	9439621	3

Table 3
With stability constraints.

INPUT		OUTPUT		
Loading Factor λ	Stability Index Limit	Stability Index L	Objective function ($/hr)	Number of Reactive Power Compensator Placements
0.05	1	0.6992	7509578	1
	0.9	0.6992	7509578	1
	0.8	0.6992	7509578	1
	0.75	0.6983	7507936	1
	0.7	0.6641	7508668	21
0.1	1	0.7284	8127704	1
	0.9	0.7284	8127704	1
	0.8	0.7284	8127704	1
	0.75	0.7164	8086343	1
	0.7	0.6299	8090264	22
0.15	1	0.7551	8934912	1
	0.9	0.7551	8934912	1
	0.8	0.7552	8938517	1
	0.75	0.7201	8726098	1
	0.7	0.6558	8730264	24
0.2	1	0.7352	9439621	3
	0.9	0.7352	9439621	3
	0.8	0.7352	9439621	3
	0.75	0.6829	9430906	3
	0.7	N/A	N/A	N/A

increasing with tightened stability index. Note that as the allowable stability index L is reduced, the stability margin i.e. the distance to the voltage collapse point (critical point) on the nose curve will increase.

An alternative corrective action to reactive power compensator placement is intentional load shedding which improves voltage stability and system voltage profile. In order to quantify the relative advantages of the two approaches, consider the results reported in [20] where the required load shedding amount is found for a feasible solution without placing any reactive power compensators. Table 4 summarizes the load shedding results for different loading factors. The cost of load shedding for a given utility can be comparatively evaluated with the cost of reactive power compensator placement in order to make investment decisions, though such analysis is beyond the scope of this work.

Table 4
Load shedding results

Loading Factor λ	Load Shedding Amount (MW)
0	47.93
0.05	82.43
0.1	117.73
0.15	153.73
0.2	190.54

Simulation-2:

The second case involves a set of 10 single line outage scenarios. In order to force the system to operate closer to its operating limits, active and reactive loads are increased by 25%. The minimum and maximum voltage magnitude limits are set at 0.9 p.u. and 1.1 p.u., respectively for all buses. Lastly, maximum reactive power injection limits of placed reactive power compensators are set as 400 MVAr. The objective of this case is to illustrate how a minimum number of strategically placed reactive power compensators can facilitate a secure and stable operation under all of the considered contingency cases.

The computational performance of the developed approach is evaluated by recording the CPU time (in seconds) for the solution of the reactive power compensator placement problem as shown in Table 5. The optimization problems are solved using Gurobi with Intel i7-8750H 2.20 GHz processor and 16 GB of RAM. It is assumed that the reported CPU times in [8] are obtained on similar computers used in this work. Furthermore, the reported timings are for only the base case without accounting for any contingencies and for a system which is significantly smaller in size than the one used in this paper. Hence, it is concluded that there is sufficient evidence implying proposed algorithm's higher computational efficiency over that of [8].

The placement results are also experimentally validated by using the Matpower optimization software [19]. It is observed that Matpower failed to yield a converged solution before placing the reactive power compensators in the system. Repeating the Matpower execution after placing reactive power compensators at the identified locations by the proposed approach, Matpower converged and yield a solution where the placed reactive power compensators provided the required reactive power to maintain voltage stability under all contingencies.

5. Conclusion

This paper is concerned about maintaining large power grids robust against a set of anticipated contingencies which may be due to extreme events or unexpected changes in generation, load or equipment failures. A two stage approach is proposed where the loose coupling between the real and reactive power problems is exploited to formulate a practical and effective method to strategically place a minimum number of reactive power compensators in the system. The proposed method is tested on a large power grid and results are validated by solving the cases using an ACOPF. The method introduces voltage profile improvements and strengthens voltage stability with modest CPU requirements even for large power grids. Future work will extend these results to more dynamic scenarios where topology and load changes in time are taken into account during an extreme event which impacts a power grid for an extended period.

CRediT authorship contribution statement

Ahmet Öner: Conceptualization, Methodology, Software, Validation, Investigation, Writing - original draft. **Ali Abur:** Conceptualization, Methodology, Investigation, Writing - review & editing, Supervision.

Declaration of Competing Interest

The authors declare that they have no known competing financial interests or personal relationships that could have appeared to influence

Table 5
SVC placement results.

No. of Solved Line Outage Scenarios	Reactive Power Compensators Placed at Bus	CPU Time (seconds)
10	2165, 2389	446.66

the work reported in this paper.

References

[1] Alhasawi FB, Milanovic JV. Techno-economic contribution of facts devices to the operation of power systems with high level of wind power integration. IEEE Trans Power Syst 2012;27(3):1414–21.

[2] Haque M. Improvement of first swing stability limit by utilizing full benefit of shunt facts devices. IEEE Trans Power Syst 2004;19(4):1894–902.

[3] Milanovic JV, Zhang Y. Global minimization of financial losses due to voltage sags with facts based devices. IEEE Trans Power Delivery 2009;25(1):298–306.

[4] Ciocia A, Boicea VA, Chicco G, Di Leo P, Mazza A, Pons E, Spertino F, Hadj-Said N. Voltage control in low-voltage grids using distributed photovoltaic converters and centralized devices. IEEE Trans Ind Appl 2018;55(1):225–37.

[5] Mansour Y, Xu W, Alvarado F, Rinzin C. Svc placement using critical modes of voltage instability. In: Conference Proceedings Power Industry Computer Application Conference. IEEE; 1993. p. 131–7.

[6] Farsangi MM, Nezamabadi-pour H, Song Y-H, Lee KY. Placement of svcs and selection of stabilizing signals in power systems. IEEE Trans Power Syst 2007;22 (3):1061–71.

[7] Azadani EN, Hosseinian S, Janati M, Hasanpor P. Optimal placement of multiple statcom. In: 2008 12th International Middle-East Power System Conference. IEEE; 2008. p. 523–8.

[8] Mínguez R, Milano F, Zárate-Miñano R, Conejo AJ. Optimal network placement of svc devices. IEEE Trans Power Syst 2007;22(4):1851–60.

[9] Chang C, Huang J. Optimal svc placement for voltage stability reinforcement. Electric Power Syst Res 1997;42(3):165–72.

[10] Pisica I, Bulac C, Toma L, Eremia M. Optimal svc placement in electric power systems using a genetic algorithms based method. In: 2009 IEEE Bucharest PowerTech. IEEE; 2009, p. 1–6.

[11] Xu X, Xu Z, Lyu X, Li J. Optimal svc placement for maximizing photovoltaic hosting capacity in distribution network. IFAC-PapersOnLine 2018;51(28):356–61.

[12] Balu NJ, Taylor CW, Maratukulam D. Power system voltage stability. McGraw-Hill; 1994.

[13] Kessel P, Glavitsch H. Estimating the voltage stability of a power system. IEEE Trans Power Delivery 1986;1(3):346–54.

[14] Allemong J, Radu L, Sasson A. A fast and reliable state estimation algorithm for aep's new control center. IEEE Trans Power Apparat Syst 1982;4:933–44.

[15] Yang Z, Zhong H, Bose A, Zheng T, Xia Q, Kang C. A linearized opf model with reactive power and voltage magnitude: a pathway to improve the mw-only dc opf. IEEE Trans Power Syst 2018;33(2):1734–45.

[16] Josz C, Fliscounakis S, Maeght J, Panciatici P. Ac power flow data in matpower and qcqp format: itesla, rte snapshots, and pegase. arXiv preprint arXiv:1603.01533, 2016.

[17] Fliscounakis S, Panciatici P, Capitanescu F, Wehenkel L. Contingency ranking with respect to overloads in very large power systems taking into account uncertainty, preventive, and corrective actions. IEEE Trans Power Syst 2013;28(4):4909–17.

[18] L. Gurobi Optimization. Gurobi optimizer reference manual, 2019. [Online]. Available: http://www.gurobi.com.

[19] Zimmerman RD, Murillo-Sánchez CE, Thomas RJ. Matpower: Steady-state operations, planning, and analysis tools for power systems research and education. IEEE Trans Power Syst 2011;26(1):12–9.

[20] Öner A, Abur A. Operating power grids during natural disasters. In: 2019 IEEE Milan PowerTech. IEEE, 2019, p. 1–6.